



**HAL**  
open science

## Faceted Gratings for an optical security feature

Qiang Song, Yoran Eli Pigeon, Kevin Heggarty

► **To cite this version:**

Qiang Song, Yoran Eli Pigeon, Kevin Heggarty. Faceted Gratings for an optical security feature. Applied optics, 2020, 59 (4), pp.910. 10.1364/AO.378122 . hal-02453810

**HAL Id: hal-02453810**

**<https://hal.science/hal-02453810>**

Submitted on 24 Jan 2020

**HAL** is a multi-disciplinary open access archive for the deposit and dissemination of scientific research documents, whether they are published or not. The documents may come from teaching and research institutions in France or abroad, or from public or private research centers.

L'archive ouverte pluridisciplinaire **HAL**, est destinée au dépôt et à la diffusion de documents scientifiques de niveau recherche, publiés ou non, émanant des établissements d'enseignement et de recherche français ou étrangers, des laboratoires publics ou privés.

# Faceted Gratings for an optical security feature

Qiang Song\*, Yoran Eli Pigeon, Kevin Heggarty

*Department of Optic, IMT-Atlantique, Technopole Brest-Iroise, CS 83818, 29285 BREST, France*

\*: [qiang.song@imt-atlantique.fr](mailto:qiang.song@imt-atlantique.fr)

**Abstract:** A method of optimizing and manufacturing a diffractive blazed grating array (DBA) is proposed to create a visual security feature when illuminated by a divergent Light emitting diode (LED) source. A pure phase grating array serving as the optical security component consists of blazed grating cells with the same size of  $75\mu\text{m}$ . After a divergent spherical wave is decomposed into harmonic-waves, each grating cell of the DBA deflects locally the harmonic-waves into predefined directions and forms a feature pattern on the target plane. Particularly, a two-step optimization method is further developed for optimizing the period and orientation of each grating cell. The DBA sample is fabricated by using our home-built parallel direct-write photo-plotter with a resolution of  $0.75\mu\text{m}$ . Both numerical simulations and optical experiments are demonstrated to validate the proposed model. Since the optical security component developed is a surface relief structure of a single polymer material, it can be replicated for mass production by using standard roll to roll nano-imprint technology. This design algorithm proposed in this work will enable the extension of the optical security elements to a broader realm and facilitate extensive developments in other research fields of the optics community, such as light shaping, specific illumination for lithography and microscope systems.  
© 2019 Optical Society of America

**Keywords:** Diffractive optics; Light shaping; Micro optics; Photo-Lithography;

## 1. Introduction

Optical security technologies have gained extensive attention in the optics community because of the distinctive visual effects of optical security components, which are widely applied in protecting documents identification, bank notes, and brands against counterfeit [1-3]. In these technologies, holography technology is the most popular anti-counterfeiting because it is almost impossible to be imitated without intensive knowledge of the specific lithography fabrication systems and design algorithms [4-6]. Although there are various technologies for making the optical security holograms, the two archetypal optical security devices are traditional optical-recording holograms and computer synthesized holograms. In these holographic based technologies, dot-matrix hologram is the most widely used technique. The dot-matrix hologram comprises many small bright dots, which are usually called ‘diffractive pixels’. In general, the diffractive pixel cannot be seen by the naked eye due to its small diameter, which is below  $80\mu\text{m}$ . The diffractive pixels are filled with diffraction gratings that can produce a 2D or 3D visual effect on the dot-matrix hologram’s surface when they are illuminated, for example by a LED source [7-9]. Another kind of dot-matrix hologram has also been presented recently, which can project a feature pattern in the far field when illuminated by a laser pointer [10]. However, a laser pointer is dangerous for human vision perception. Thus, there is an important opportunity for projecting a feature pattern with a safer source (such as LED available for example on all smartphones). We aim to use pure phase diffractive optical element (PDOE) arrays to design such a device.

The problems of PDOE designs have been studied extensively in many publications over the past forty years [11-15]. Mathematically, the optimization of a PDOE is equivalent to solving an inverse problem [16-18]. The mainstream method for designing most PDOEs is the famous three-step iterative Fourier transformation algorithm [12]. However, PDOEs usually require a collimated light source. To address this issue, a recent research devoted to divergent light shaping was proposed [19]. Although it is still a heavy computation work to design such kind of PDOEs, the number of sampling points will become large when illuminated with divergent light. It indicates that the approach is not the most suitable for divergent light sources.

One solution for LED light shaping is based on the element cells method, which has been introduced recently [20]. Nevertheless, this letter did not disclose the optimization and fabrication methods, or give real experimental results. Therefore, efficient design algorithms and fabrication methods enabling light manipulating illuminated by divergent light source is highly required.

Here, we present a cost-efficient design algorithm and a fabrication method to produce a new kind of diffractive blazed grating array (DBA) which can solve the problems imposed by the divergent LED source. As far as we know, this is the first time reported in security hologram community. A two-step iterative optimization algorithm is proposed to optimize each grating cell's parameters and improve the fabrication performance. Then, a DBA sample is fabricated by using our home-built parallel gray scale direct-write photo-lithography machine [21-22]. To verify the proposed design algorithm, both simulations and optical experiments are performed. The design model and optimization algorithm are described in detail in Section 2. The numerical simulations, fabrication results and experiment results are presented in Section 3. The results are discussed in Section 4. Finally, we conclude our work in Section 5.

## 2. Principle

### 2.1 Diffraction theory of the blazed grating array

The functional principle schematic is shown in Fig.1.

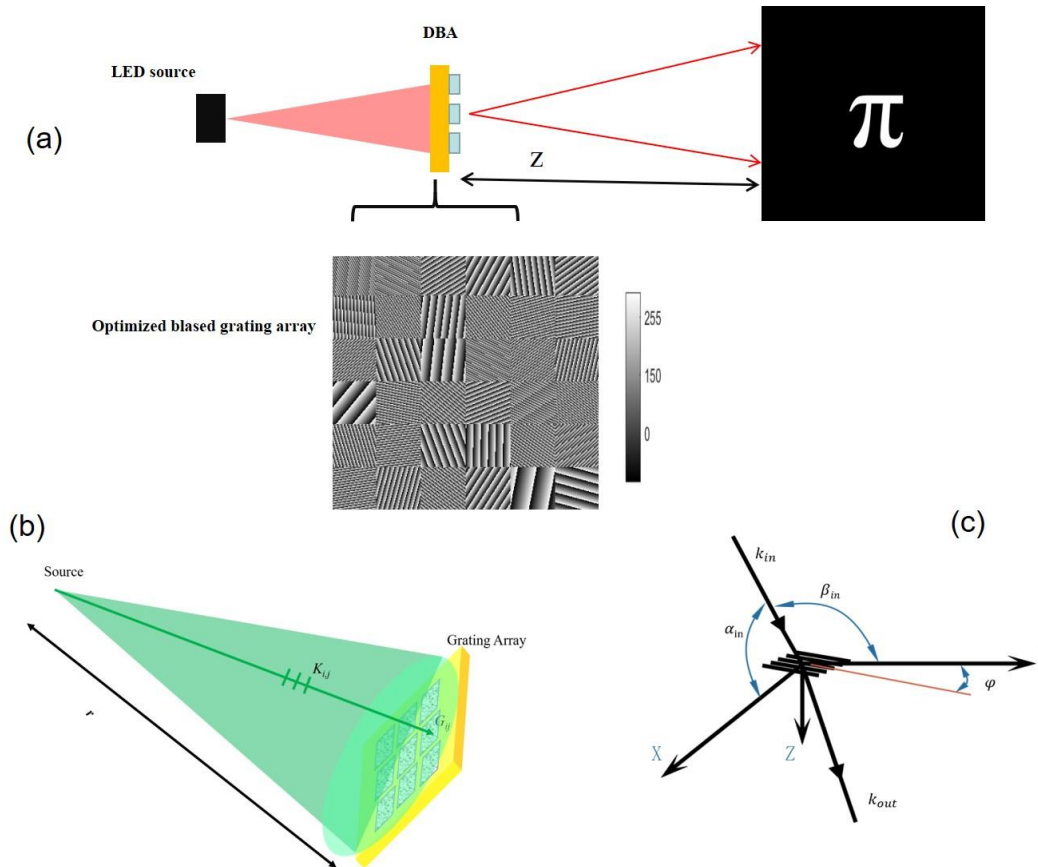


**Fig.1** (a)The schematic of the DBA principle for producing arbitrary patterns. (b) Schematic of the spherical wave decomposition. (c) Arrangement of vector  $k_{in}$  and  $k_{out}$

In Fig.1(a), the DBA consists of an array of blazed gratings cells, where each grating cell has designated spatial period  $P$  and orientation angle  $\varphi$ . A diffraction pattern is obtained from the superposition of the first

diffraction order of each blazed grating when illuminated by a narrow spectrum divergent LED source. A diffraction pattern, is projected onto a screen at a distance  $z$ . Usually, the distance is much larger than the period  $P$ , thus the diffraction result can be described by scalar Fresnel diffraction. In our case, we choose blazed gratings because the multi-level blazed grating can obtain high diffraction efficiency in the first order.

From Fig.1(a), the electric field  $U_{out}(X,Y)$  of the target plane can be described in Eq.(1).

$$E(X, Y) = e^{jk\frac{X^2+Y^2}{2z}} FT(E_{in}e^{jk\frac{x_0^2+y_0^2}{2z}}) \quad (1)$$

In eq.(1), the FT means the Fourier transform,  $z$  is the distance between the DBA plane and target plane,  $(x_0, y_0)$  and  $(X, Y)$  represent the orthogonal coordinates of in the DBA plane and target plane. The blazed grating introduces a linear phase shift of the wave-front, and the light incident on each grating cell is modelled as a divergent spherical wave. Based on the thin-element approximation approach, the electric field behind each grating cell can be expressed as:

$$E_{in} = \frac{A}{r} e^{\frac{jkr}{r}} e^{j(k_x x_0 + k_y y_0)} \quad (2)$$

Where  $A$  and  $k$  represent the amplitude and wave vector of the incident light, and  $r$  is the distance from source to the DBA.  $k_x$  and  $k_y$  are the grating vectors in X and Y directions, respectively. The incident spherical wave can be divided into lots of plane wave, as shown in Fig.1(b). Here,  $K_{ij}$  means the wavevector at the (i,j)-th grating,  $G_{ij}$  represents the (i,j)th grating. If each grating cell is small enough, the wave on each unit can be approximated as a plane wave. The incident angle on each grating cell is expressed as shown in eq.(3)

$$\theta_{ix} = \tan^{-1} \frac{x_i}{r}, \quad \theta_{iy} = \tan^{-1} \frac{y_i}{r} \quad (3)$$

In eq.(3),  $x_i$  and  $y_i$  are the global coordinates of each grating cell's center, and  $r$  is the distance between light source and the diffractive element. In the case of a single grating, let us consider an arbitrary grating cell of the optical element. Fig.1(c) depicts the schematic of the divergent light incident onto the grating cell (wave vector  $k_{in}$ ) and the light diffracted from the grating cell toward the target plane (wave vector  $k_{out}$ ). The absolute values of vector  $k_{in}$  and  $k_{out}$  are the same, equal to  $2\pi/\lambda$ , but the directions are different. Here,  $\lambda$  is the design wavelength.

The coordinates  $k_{in}$  of each grating cell are known, so the direction cosine of the incident light can be calculated. The grating's conical diffraction formalism is described as below,

$$\alpha_{out} + \alpha_{in} = \frac{m\lambda}{P} \sin\varphi, \quad \beta_{out} + \beta_{in} = \frac{m\lambda}{P} \cos\varphi \quad (4)$$

In eq.(4), the  $\alpha_{in}$ ,  $\beta_{in}$  are direction cosine of incident light in  $x$  and  $y$  directions, respectively, and  $m$  is the diffraction order, in this work,  $m=1$ .  $\alpha_{out}$ ,  $\beta_{out}$  are direction cosine of output light in  $x$  and  $y$  directions, respectively. Parameter  $P$  is the period of the current grating cell, and  $\varphi$  is the grating's orientation angle (See Fig.1(c)). Consequently, the angular position of a single point on the target plane is controlled by the spatial period and orientation angle  $\varphi$  of the individual grating cell. Based on Eq.(1)-(4), the period and the orientation angle of each grating can be optimized iteratively, until the desired irradiance distribution is obtained on the target plane.

## 2.2. Algorithm Description

The iteration flowchart is shown in Fig.2. The detail process is described below, and this algorithm is divided into two parts. In the first part, the initial parameters are obtained by implementing an iterative method. The second part of the proposed algorithm reduces the maximum diffraction angle of DBA. The second part is very important, because it improves the fabrication performance: the bigger period of the grating cell, the better fabrication quality. Here, we use a binary target pattern “ $\pi$ ”

to design the algorithm. The DBA has a total size of  $M \times N$  (rows x columns) pixels. The maximum target intensity can be recorded as “1”, and the size of the target pattern is  $P \times Q$ . The total number of the grating cell  $K$  should be larger than  $P \times Q$  to get the correct target pattern. Mathematically, it is an inverse problem to obtain each grating cell's parameters. The inverse problem thus reduces to calculating the grating function matrix  $G$  from equation  $\Gamma G = F(x, y)$ . Here, the operator  $\Gamma$  represents the diffraction propagation in Eq.(1), and  $F(x, y)$  represents the target matrix. Grating matrix  $G$  can be defined as below in eq.(5). The element  $G_{i,j}$  is written as  $(\varphi_{ix}, \varphi_{jy})$ .

$$G = \begin{bmatrix} G_{11} & \cdots & G_{1N} \\ \vdots & \ddots & \vdots \\ G_{N1} & \cdots & G_{NN} \end{bmatrix} \quad (5)$$

The iterative optimization reduces the residual function  $\|\Gamma G - F\|$ . For each target point, the corresponding number of grating cells can be calculated as  $K = M \times N / (P \times Q)$ . At the beginning, the initial orientation angle of each grating cell is set randomly. The orientation angle of each cell's grating can be written as :

$$\varphi_{ix}^0 = \frac{\varphi_{max}}{N} (i + rand) \quad (6)$$

$$\varphi_{jy}^0 = \frac{\varphi_{max}}{N} (j + rand) \quad (7)$$

Considering the high diffraction efficiency requirement, blazed gratings are used. The initial transmission function of each blazed grating cell can be expressed as

$$t_{ij}(x_0, y_0) = e^{i\frac{2\pi}{P}(cos\varphi_{ix}^0 + sin\varphi_{iy}^0)} \quad (8)$$

Combining eq.(1) , (2) and eq.(8), the diffractive field for divergent light source is calculated as

$$E_t = \sum_{i,j}^{N,N} e^{jk\frac{x^2+y^2}{2r_{i,j}}} FT[e^{j(k_{in,x}^i x_0^i + k_{in,y}^j y_0^j)} t_{i,j}(x_0^i, y_0^j) e^{jk\frac{x_0^{i2} + y_0^{j2}}{2r_{i,j}}} ] \quad (9)$$

In eq.(9), the  $X, Y$  are the global coordinates in  $X$  and  $Y$  directions in the target plan.  $x_0^i$  and  $y_0^j$  are the local coordinates in the  $x_0$  and  $y_0$  directions of grating cell  $G(i,j)$ , respectively. The divergent light source can be decomposed into harmonic plane waves in  $K$ -space, see Fig.2. So,  $e^{j(k_{in,x}^i x_0^i + k_{in,y}^j y_0^j)}$  is regarded as a plane wave of the coordinate index  $(i, j)$  cell, and the merit function on the target plane can be defined as

$$MSE = \frac{\sum_{N,N} \sum (I_t - I_{target})^2}{NxN} \quad (10)$$

In eq.(10),  $I_t = E_t * conj(E_t)$  is the output pattern obtained at the current iteration number. When the intensity of certain point on target plane is lower than the target value, its corresponded grating cell's coordinate index is fixed and stored for the current iteration. Otherwise, its corresponding grating index is abandoned. When all the grating cell's indices are found, we can fix this cell's matrix, and begin the next iteration. Here, we define “ $S$ ” matrix as a storage matrix to store the fixed grating cell's indices. So, the orientation matrix can update as following equations.

$$\varphi_{ix}^k = \varphi_x(i, j)^{k-1} S(i, j) + [1 - S(i, j) \frac{\varphi_{max}}{N} (i + rand)] \quad (11)$$

$$\varphi_{jy}^k = \varphi_y(i, j)^{k-1} S(i, j) + [1 - S(i, j) \frac{\varphi_{max}}{N} (i + rand)] \quad (12)$$

The new updated orientation angle of each grating cell will enter into the next iteration. This iteration process ends when the merit function value is accepted or the maximum iteration number is reached. The results of the first step optimization are not the optimal solutions, while cells with high diffraction angle grating should have their diffraction angles reduced to improve fabrication performance. To do this, the second step of the proposed algorithm is executed which we call the exchange method.

To clearly understand this exchange method, the flowchart and schematic of the exchange method are shown in Fig.3. The details of the second optimization process are summarized below.

1. Calculate the current diffraction angle of each grating cell, and find out the maximum one marked with  $C_{max}$ , the grating cell  $C_{max}$  corresponds to the target point  $T_{max}$  in target plane, see Fig.3 .
2. Calculate the diffraction angles between the current target point  $T_{max}$  and all other grating cells, then sort their value from smallest to largest.
3. Swap the grating cell  $C_{max}$  and grating cell  $C_i$ , that means let the grating cell  $C_{max}$  corresponds to target point  $T_i$ , and the grating  $C_i$  correspond to target point  $T_{max}$  .
4. Check the diffraction angle value after exchange:
  - a) If the new diffraction angle is not smaller than the current grating cell  $C_{max}$ , the exchange is cancelled, then swap the  $C_{max}$  with the next grating cell, until all the remaining grating cells are exchanged.
  - b) If the updated diffraction angle is decreased after exchange, the algorithm goes to step 5.
5. If the exchange of current grating cell  $C_{max}$  doesn't happen, the algorithm ends. If the exchange happens, the algorithm goes to step 1, and updates the  $C_{max}$ .

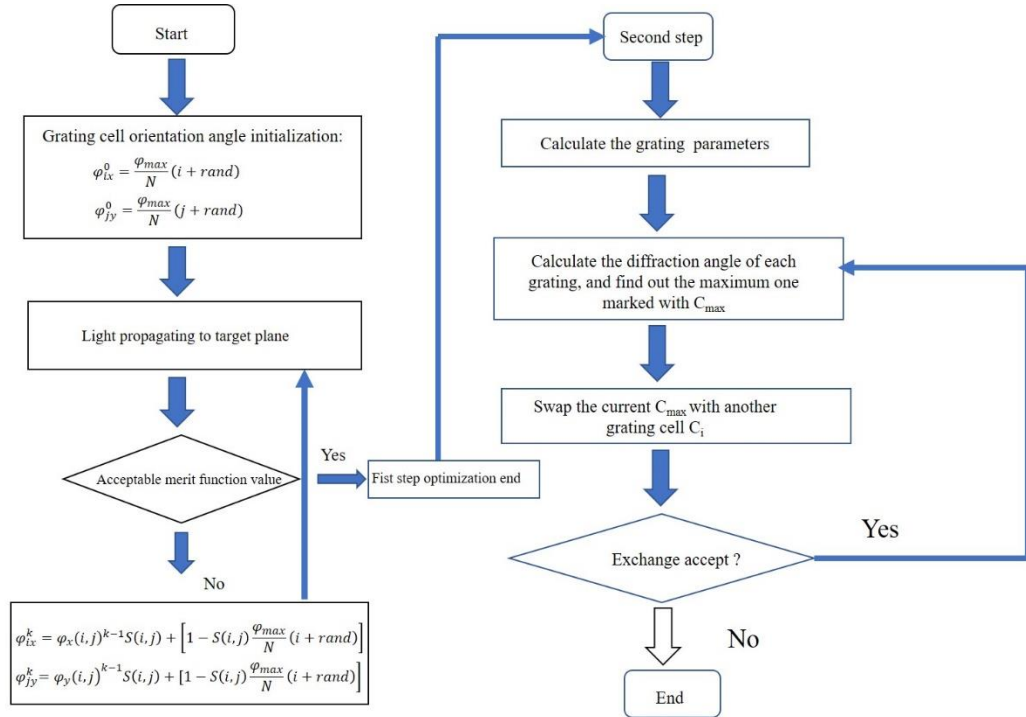


**Fig.2.** Flowchart of the first part of DBA design algorithm

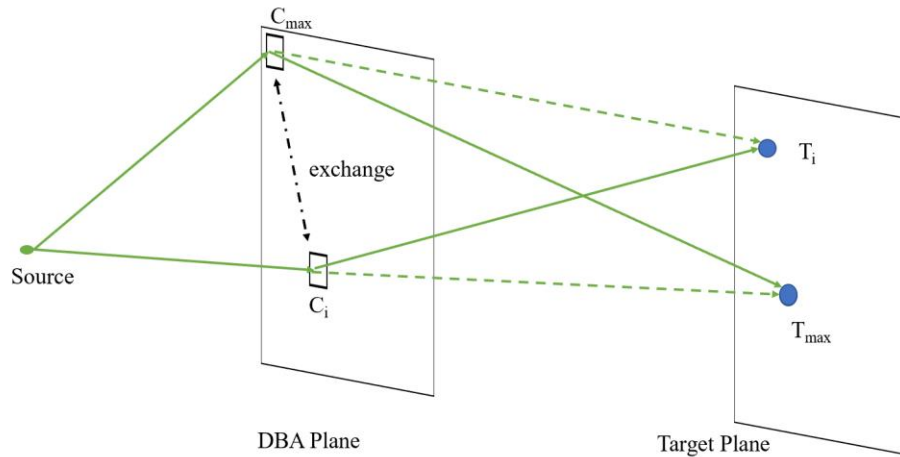


**Fig.3.** Schematic of the diffraction angle optimization. The solid lines are the rays before exchange, and the dotted line are the optimal rays after exchange

### 3. Numerical Simulation and Experiment Results

#### 3.1 Numerical Simulation

In order to verify the feasibility of the proposed design method, we perform the numerical simulations. To reduce calculation time, a binary pattern “ $\pi$ ” with image size  $40 \times 40$  pixels was used to verify the design method in the numerical simulation. The target is shown in Fig.4. In this simulation test, considering the computation amounts, pixel size of each grating cell is  $3\mu\text{m}$ , and the resolution of each grating cell is  $60 \times 60$  pixels as the number of a cell is  $30 \times 30$ . The total size of DBA is  $5.4\text{mm} \times 5.4\text{mm}$ . A  $525\text{nm}$  wavelength LED is used as the light source, here, the distance from source to DBA plane is  $100\text{mm}$ , this distance cannot be too far because the energy from the divergent light source decrease rapidly. The propagation distance is  $200\text{mm}$  from DBA to target plane.

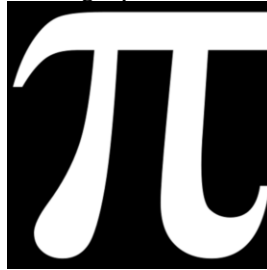


**Fig.4.** The target image for DBA design.

The final numerical simulation results with these parameters are demonstrated in Fig.5. The maximum diffraction angle against the number of exchanges is plotted in Fig.5(a). The final optimal phase map of The diffracted reconstructed result is implemented in VirtualLab Fusion™ software [20] to verify the proposed method, which is shown in Fig.5(b). From Fig.5 (b), as we should see the speckle noise because we implement this numerical field tracing with a divergent coherent light source in VirtualLab Fusion software. These speckle noises will be suppressed when the low coherence degree LED source is used in real experiment.

To further verify the proposed design method, the real experiments are performed to verify the proposed DBA computation method.

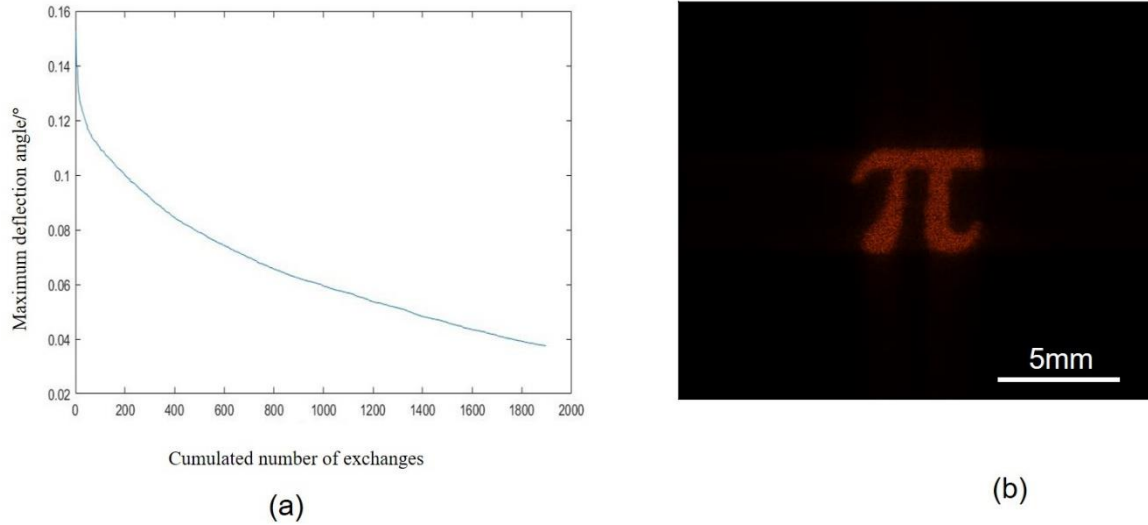


**Fig.5.**The numerical simulation results.(a)Maximum deflection angle against the cumulated number of exchanges; (b) Reconstructed result in VirtualLab Fusion™ software.

### 3.2 Fabrication and Experimental Results

With the algorithm mentioned above, a DBA was designed with 200\*200 grating cells, each grating cells was 100\*100 pixels with pixel size of 0.75 $\mu$ m, and the collective divergent angle is about 16 degrees. The total calculation time is about 10 minutes on a personal computer (Intel Core™ I7-8750H CPU@2.2GHz, GPU GTX1060). According to the proposed method in Section 2.2, the maximum diffraction angle can be reduced, as show in Fig.6.

The fabrication facilities we used to make DBA are our home-built direct-write photo-plotter [21-22]. In this experiment work, the photoresist is S1813 from Mirco Resist Technology, and the refractive index is 1.66 at a wavelength of 525nm. There are three steps to fabricate the DBA. For more detailed fabrication descriptions, we suggest the readers refer to our previous work[23]. Fig.7(a) shows fragments of the grating cell array, which are captured by a microscope (Reichert-Jung Polyvar Met). The height profile of single cell obtained by an interference microscope( Nikon Optihot100) can be seen in Fig.7(b). The height of the fabricated grating is about 750nm, it is not exactly with the designed height due the fabrication errors. This depth error decreases the diffraction efficiency. To know how it affects the diffraction efficiency, the diffraction efficiency as function of the grating depth is calculated based on rigorous coupled wave analysis (RCWA)[24-25], as shown in Fig.7(c). The calculated diffraction efficiency of first order is near to 90% for a depth of 750nm. An experiment to measure the grating's first order diffraction efficiency was also implemented. The experimental first order diffraction efficiency is about 82%, where it has 6% difference with the theoretic computation, and the error comes mainly from the Snell reflection loss of the glass.



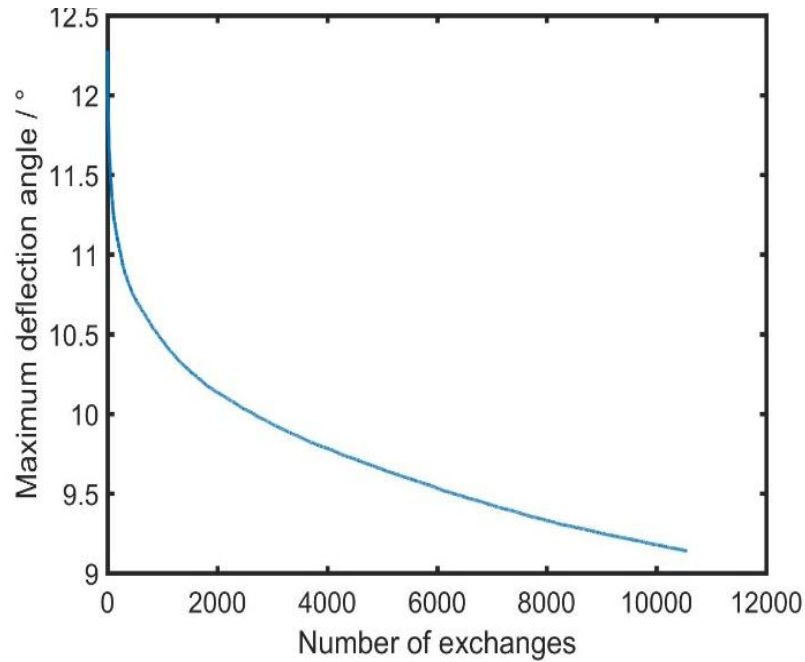


Fig.6. Maximum deflection angle against with the cumulated number of exchanges of the real DBA

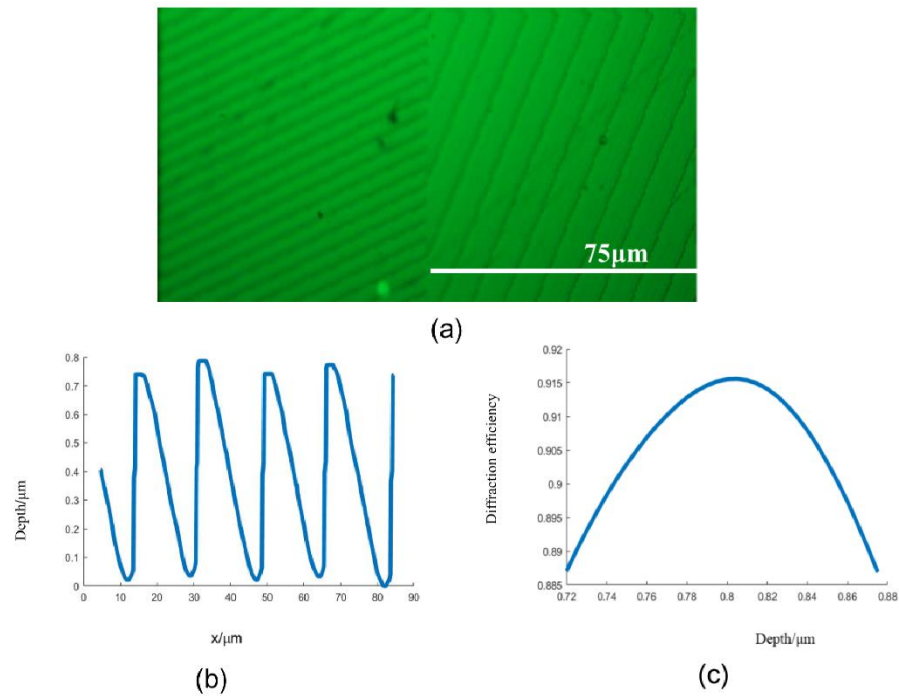
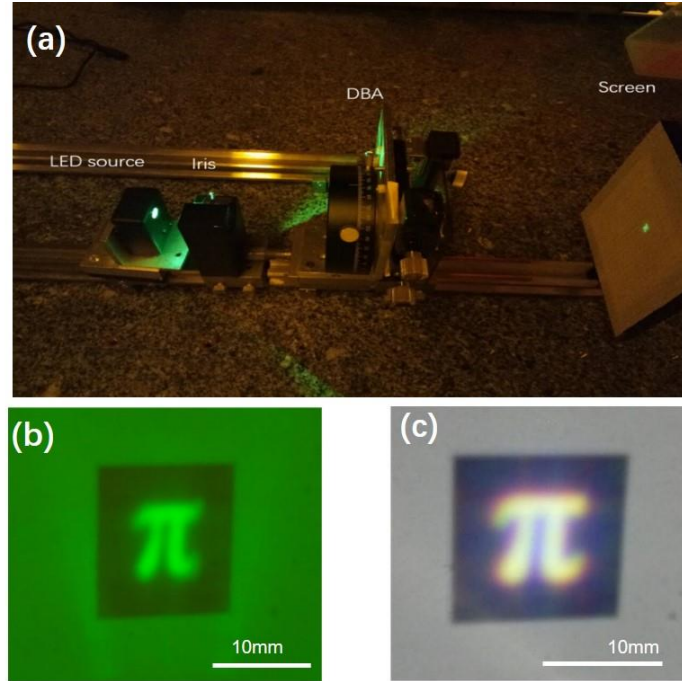


Fig.7.Surface structure and surface profile. (a)Fragments of the fabricated grating cell array; (b). Height profile of single fabricated grating cell;(c).Normalized first order diffraction efficiency against depth.

Fig.8(a) is the experiment setup to show the result, it consists of a LED source, the iris, the DBA and the screen. Here, the iris is used to block other non-useful light. When the DBA is illuminated by a green LED source, the reconstructed pattern is obtained as shown in Fig.8(b). A reconstructed image illuminated by

white light LED of a smart-phone is also presented in Fig.8(c), the feature pattern can still be recognized with less color dispersion. The experiment results can prove that the proposed method is available in optical security hologram.



**Fig.8.**(a) Experiment setup; (b) The intensity distribution on the target plane as a result of illuminating the DBA with a green LED source;(c)Intensity distribution on target plane when illuminated by white a LED of a smart-phone.

#### 4. Discussion

This paper has focused on an optimization algorithm to design blazed grating array structures for using under incoherent divergent illumination particularly suited to security hologram applications. The experimental results demonstrate that the proposed functions well. However, for this to be the case, a number of interdependent optical system parameters must be chosen correctly. Such parameters include source-DBA distance, DBA size and grating cell size. We are discussing how these different and sometimes conflicting factors affect design, with the aim of providing some simple design guidelines for optical engineers.

The most important overall consideration is to maintain the blazed grating period of the individual cells within the bounds imposed by their performance and fabrication limits. The second optimization step of the proposed algorithm helps toward this aim, whereas system design is also very important. Fig.9(a) shows the first order diffraction efficiency of a blazed grating against grating period with normal incidence. Fig.9(b) shows the dependence on grating groove depth (a good guide to DBA fabrication and replication accuracy) and incident illumination angle by keeping the grating's spatial period. Both figures are based on RCWA model because the thin element approximation scalar theory is no longer accurate for small grating periods and off-normal illumination. Clearly, to maintain high diffraction efficiency (greater than 85%), grating period should be greater than roughly  $5\mu\text{m}$  and incident angles should be less than about 10 degrees. These considerations have a direct influence on usable DBA sized and source-DBA distances: a DBA with lateral dimensions of the order of cm should be illuminated by a source at a distance of tens of cm. These values are perfectly compatible with our security hologram application. Of course, the further the DBA is placed from a divergent source, the less light it will capture to reduce the intensity of the diffracted image. The optimal DBA size and position will thus be an engineering compromise based on these competing factors.

Another important system design consideration is the DBA size. If the cell is too large, we can no longer approximate the light from the divergent source to be a plane wave across the cell. If the cell is too small, the diffracted spot size (resulting by the cell aperture) in the output image will increase in size, limiting the complexity and resolution of the output image. The output intensity distribution of each spot is given by

$$D_{spot} = d^2 \text{sinc}\left(d \frac{x}{\lambda z}\right) \text{sinc}\left(d \frac{y}{\lambda z}\right) \quad (13)$$

In eq. (13),  $d$  is the size of the grating cell,  $z$  is the distance between DBA and image plane, and  $\lambda$  is the wavelength. With the DBA sizes and distances indicated above, cell dimensions on the order of 100 $\mu\text{m}$  offer a good engineering compromise, with the added advantage that the cells are then barely visible by direct eye observation.

A final consideration is DBA performance with non-monochromatic divergent sources such as readily available smartphone white LEDs. The LED used in our experimental system (Fig. 8) had a measured Full width half maximum spectral width 33nm. Fig. 9(c) shows that over such spectrum ranges the diffraction efficiency of the blazed grating varies very little. For a white LED, the wavelength variation of grating diffraction angle and diffraction efficiency produces colour fringing in the output pattern. However, as system design considerations and the algorithm optimization tend to keep diffraction angles low (<10 degrees), these effects are limited and the desired pattern remains clearly recognizable, see Fig. 8(c).

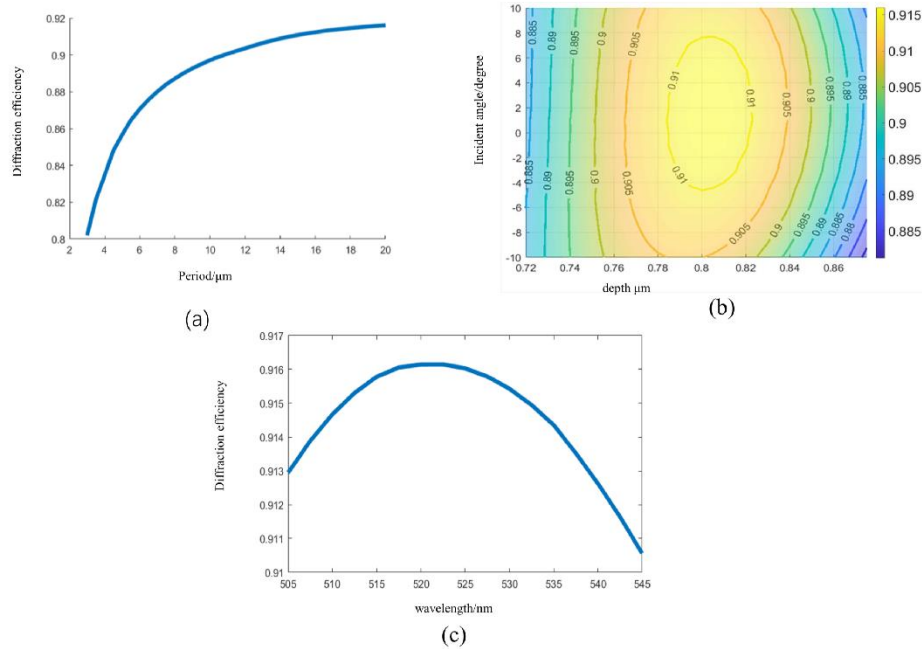


**Fig.9.** (a) The calculated first order diffraction efficiency as a function of grating period obtained by RCWA; (b) Diffraction efficiency against wavelength; (c) The calculated first order diffraction efficiency as a function of grating groove depth and incident angle obtained by RCWA.

## 5. Conclusion

In this paper, DBA method for optical security hologram application is presented. The grating parameters of each cell are obtained by using the proposed two-step optimization algorithm. The fabrication process has been introduced, and the DBA was fabricated with our home-built parallel maskless photolithography machine. The fabricated sample and experiment results prove that the proposed method is feasible. Meanwhile, the diffraction efficiency can achieve 82% at the first diffraction order with blazed grating. The factors which can affect the design result are also demonstrated in Section 4, where it can give an optical engineer a design guide. Our method can provide a feasible way not only in optical security device with simple surface profile compared with traditional DOE, but also in optical fields requiring functional illumination such as photo-lithography and microscopy.

## Acknowledgments

This work is supported by the European Union's Horizon 2020 research and innovation program through PHENomenon under grant agreement No.780278 and Brest Metropole Ocean.

## Disclosure

The authors declare no conflicts of interest.

## References

1. R. L. Van Renesse, *Optical Document Security* (Artech House, 2005).
2. L. C. Ferri, "Visualization of 3D information with digital holography using laser printers," *Comput. Graph.* **25**(2), 309–321 (2001).
3. B. Gu, "Review - 40 years of laser-marking - industrial applications," *Proc. SPIE* **6106**, 61061(2006).
4. Fernando da Cruz Vasconcellos, Ali K. Yetisen, Yunuen Montelongo, Haider Butt, Alexandra Grigore, Colin A. B. Davidson, Jeff Blyth, Michael J. Monteiro, Timothy D. Wilkinson and Christopher R. Lowe, "Printable Surface Holograms via Laser Ablation," *ACS Photonics* **1**(6), 489–495(2014).
5. Alexander. Goncharsky, Anton. Goncharsky, and S. Durlevich, "Diffractive optical element with asymmetric microrelief for creating visual security features," *Opt. Express* **23**(22), 29184–29192 (2015).
6. Kevin T.P. Lim, Hailong Li, Yejing Liu and Joel K.W. Yang, "Holographic colour prints for enhanced optical security by combined phase and amplitude control," *Nat. Commu* **10**(25), 2019.
7. Anton Goncharsky and Svyatoslav Durlevich, "cylindrical computer-generated hologram for displaying 3D images ," *Opt. Express* **26**(17) 22160-22167(2018)
8. Alexander Goncharsky, Anton Goncharsky, and Svyatoslav Durlevich, "Diffractive optical element for creating visual 3D images," *Opt. Express* **24**(9) 9140-9148(2016).
9. An. Firsov, A. Firsov, B. Loechel, A. Erko, A.Svintsov, and S.Zaitsev, "Fabrication of digital rainbow holograms and 3-D imaging using SEM based e-beam lithography," *Opt. Express* **22**(23) 28756-28770(2014).
10. M.S.Khan, Maik Rehlves, Roland Lachmayer, and Bernhard Roth, "Polymer-based diffractive optical elements for rear end automotive applications: design and fabrication process," *Appl. Opt.* **57**(30) 9106-9113(2018).
11. R.W. Gerchberg and W. O. Saxton, "A practical algorithm for the determination of the phase from image and diffraction plane pictures," *Optik* **35**(2), 237-246(1972).
12. Frank Wyrowski, "Diffractive optical elements: iterative calculation of quantized, blazed phase structures," *J. Opt. Soc. Am. A* **7**(6), 961-969(1990).
13. Kevin Heggarty, Raymond Chevallier, "Signal window minimum average error algorithm for computer-generated hologram," *J.Opt.Soc.Am.* **A15**(3), 625-635(1998).
14. Marwa Elbouz, Kevin Heggarty, " Signal window minimum average error algorithm for multi-phase level computer-generated holograms," *Opt.Comm.* **18**(1-3), 21-28(2000).
15. L.Kelemen, S.Valkai and P. Ormos, "Parallel photopolymerization with complex light patterns generated by diffractive optical elements,"*Opt.Express* **15**(22),14488-14497(2007)
16. Haichao Wang, Weirui Yue, Qiang Song, Jingdan Liu, Guohai, Situ, " A hybrid Gerchberg-Saxton-like algorithm for DOE and CGH calculation," *Opt Laser Eng.* **89**(2), 109-115(2017)
17. J.R. Fienup and C.C.Wackerman,"Phase-Retrieval Stagnation Problems and Solutions," *J.Opt.Soc.Am. A* **3**(11), 1897-1907(1986).
18. J.H.Seldin and J.R.Fienup, "Numerical Investigation of the Uniqueness of Phase Retrieval ," *J.Opt.Soc.Am. A* **7**(3), 412-427(1990).
19. Qiang Song, Yoran Eli Pigeon , Xavier Theillier, Kevin Heggarty, " An optimization approach of computer generated hologram for divergent light shaping," *Digital Holography and Three -Dimensional imaging*, 2019.
20. Daniel Asoubar, Christian Hellmann, Hagen Schweitzer, Michael Kuhn, Frank Wyrowski, "Customized homogenization and shaping of LED light by micro cells arrays," *Proc. SPIE* **93831B**(2015).
21. M.V.Kessels, K.Heggarty, "Optical proximity correction for a versatile LCD based direct write maskless photoplotter," *Opt.Comm.* **86**(12), 2385-2391(2009).
22. M.V.Kessels, C.Nasour,P.Grosso, K.Heggarty, " Direct write of optical diffractive elements and planar waveguides with a digital micromirror device based UV photoplotter," *Opt.Comm.***283**(15), 3089-3094(2010).
23. Qiang Song, Yoran Eli Pigeon, Kevin Heggarty, "Faceted Fresnel DOEs creating the perception of a floating 3D virtual object under divergent illumination," *Opt.Comm.***451**(15), 231-239(2019).
24. M.G.Moharm, Eric B. Grann, Drew A.Pommet, and T.K.Gaylord, "Formation for stable and efficient implementation of the rigorous coupled-wave analysis of binary grating,"*J.Opt.Soc.Am.***A12**(5),1068-10276(1995).
25. Lifeng Li, "Use of Fourier series in the analysis of discontinuous periodic structures," *J. Opt .Soc Am* **A13**(9), 1870–1876(1996).